CMOS-compatible wavefront detector

D. W. de Lima Monteiro and G. Vdovin

Electronic Instrumentation Laboratory, ITS /DIMES, Delft University of Technology

Mekelweg 4, 2628 CD Delft, The Netherlands, tel./fax:+31 15 278 6285/5755

davies@titus.et.tudelft.nl

ABSTRACT

We report on the development of an integrated Hartmann-Shack wavefront detector implemented in the framework of a standard Complementary-Metal-Oxide-Semiconductor (CMOS) technology, the most used for Integrated Circuit (IC) fabrication nowadays. The detector consists of an array of 8x8 addressable quad-cells, an analog demultiplexer and a sampling-rate controller integrated on-chip, and a customized microfabricated Hartmann mask to sample the incident optical wavefront. The role of the sensor is to sense aberrations present in a light beam.

RESUMO

Neste artigo abordaremos o desevolvimento de um detector de frentes de onda integrado do tipo Hartmann-Shack, implementado em tecnologia CMOS padrão, hoje em dia a mais usada para fabricação de circuitos integrados (CIs). O detector consiste em uma matriz com 8x8 células quadrante, um multiplexador analógico e um controlador de amostragem embutidos no chip, além de uma máscara sob medida do tipo Hartmann e microfabricada, utilizada para amostrar a frente de onda óptica incidente. O papel desse sensor é detectar aberrações presentes em um feixe de luz.

***Key words* —** Wavefront sensor, CMOS, adaptive optics, position sensing.

I. INTRODUCTION

The overwhelming growth of the computer manufacturing and microelectronic products led to a widely spread availability of complementary-metal-oxide-semiconductor (CMOS) foundries, intense research on related devices and mature integrated circuit (IC) design methods and simulators.

Recently, several companies and research institutes worldwide have been exploiting the optical detecting properties of CMOS devices to compete with traditional CCD's [1]. An optical device implemented in CMOS can have a number of embedded functions due to its IC compatibility.

No optical system is completely aberration-free and some propagation media introduce distortions to an originally perfect wavefront passing through them. In order to obtain some optical quality at the end of the optical path, a way to compensate for the aberrations is required.

Adaptive Optics (AO) is a relatively new branch of optics that deals with sensing and correction of aberrations present in optical wavefronts [2]. These actions are performed by two main components in an AO system, i.e., a wavefront sensor (WFS) and an adaptive corrector [3, 4], respectively. The aberration information collected by the first is passed to the latter, which extracts the aberration components of the wavefront.

Several techniques to measure wavefronts have been devised so far [5]. The curvature and the Hartmann-Shack method are the most widely used ones. The curvature method, however, is only capable of operation in close-loop (coupled to an adaptive corrector), whereas the Hartmann-Shack one allows the wavefront sensor to be employed 'solo' as a diagnostic tool, as for laser-beam diagnostics and human-eye aberration estimation.

Although Hartmann-Shack (H-S) sensors already exist, they are either expensive, bulky or slow (mostly lower than 100 Hz), and in many cases feature a combination of the aforementioned factors. These can be limiting factors to the use of adaptive optics in a number of applications. Therefore, we have implemented a cost-effective, fast and integration-friendly wavefront sensor.

II. THE WAVEFRONT SENSOR

An H-S wavefront sensor has a straightforward principle of operation. As can be seen in Fig.1, a reference wavefront propagating from left to right is sampled by a microlens array. This causes light spots to be present at reference positions on the focal plane, where a detector is positioned. The spot centroid reference positions are recorded and stored. If an aberrated wavefront is then input to the sensor, the local tilt at each microlens (as a result of integration of high-frequency tilts over each site) causes a displacement of the spot position, in relation to the reference one.

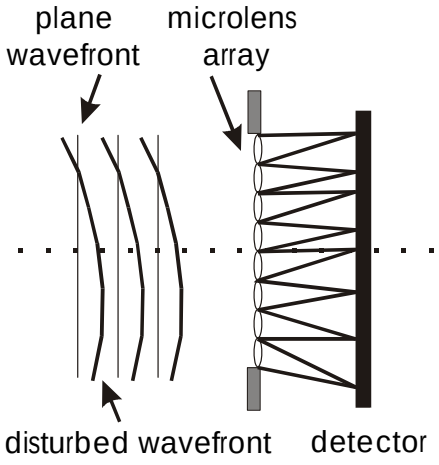

Fig. 1. Schematics of a Hartmann-Shack WFS

There is a direct relation between the spot displacements and the deviation of the tested wavefront from the reference one, as indicated in (1) and (2).

$$dx = f\,\frac{\partial W}{\partial x} \tag{1}$$

$$dy = f\,\frac{\partial W}{\partial y} \tag{2}$$

Where dx and dy are the spot displacements in the respective directions, dW_x and dW_y are wavefront tilts for each coordinate and f is the microlens focal length.

One is therefore able to reconstruct the wavefront, visualize it graphically and obtain the contributions of various well-known aberrations (as defocus and astigmatism) to the complex distortion. This can be done by decomposition of the vector of position displacements over an orthogonal basis [1, 6].

III. POSITION-SENSITIVE DETECTORS

To compute the displacements of the spots a position detector capable of dealing with multiple spots must be used. One solution is to use an imager, so that an image frame is grabbed and a special data-reduction algorithm reduces the bitmap into coordinate information. This, however, requires considerable processing time.

On the other hand, a matrix of optical position-sensitive detectors (PSD's) can be used, where each PSD is associated with one spot. There are several different layouts for a PSD [7, 8], from which we chose a quad-cell (QC), as depicted in Fig.2, due to its well-defined center, absence of a resistive network and high fill factor, compared to counterparts of the same size. Although a QC only provides a linear response in its very central part, the overall response is well behaved and once mapped, can lead to solely noise-limited position information.

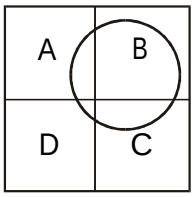

Fig. 2. Circular spot on a quad-cell (QC) with four photodiodes

The main advantage of using a PSD is that information on the spot centroid position is readily available after extremely simple mathematical calculations on its output signals, which overcomes the image processing and increases operational speed of the WFS. Equations (3) and (4) show the QC response as a function of the four cells output signals.

$$x_{QC} = \frac{(I_B + I_C) - (I_A + I_D)}{I_A + I_B + I_C + I_D} \quad (3)$$

$$y_{QC} = \frac{(I_A + I_B) - (I_C + I_D)}{I_A + I_B + I_C + I_D} \quad (4)$$

IV. Implementation of the Device

A. Light sampling plane

Instead of a microlens array we chose to use a Hartmann mask, which is an orthogonal array of apertures. Although the incoming wavefront is partially blocked, it is sampled at known positions and that allows its reconstruction.

Sixty-four 450μm circular apertures, with a 1000μm pitch, were etched on a 1.1μm thick Aluminum layer deposited on a glass substrate.

B. Detector

The detector was implemented in a 1.6μm double-metal single-poly n-well analog CMOS process. Digital circuitry has been isolated from analog circuitry by using guard rings in order to minimize substrate interference.

The sensor consists of an orthogonal array of 256 pixels, clustered 4x4 so to feature 64 quad-cells. A 6-bit analog demultiplexor manages the analog data flux from each addressed pixel to the output bus. The sampling-rate controller can be instructed to either let a single QC or a pair of QC's be addressed at a time, allowing either 4 or 8 outputs per address. A diagram of the chip is presented in Fig. 3. The effective detector area is 8 mm x 8 mm.

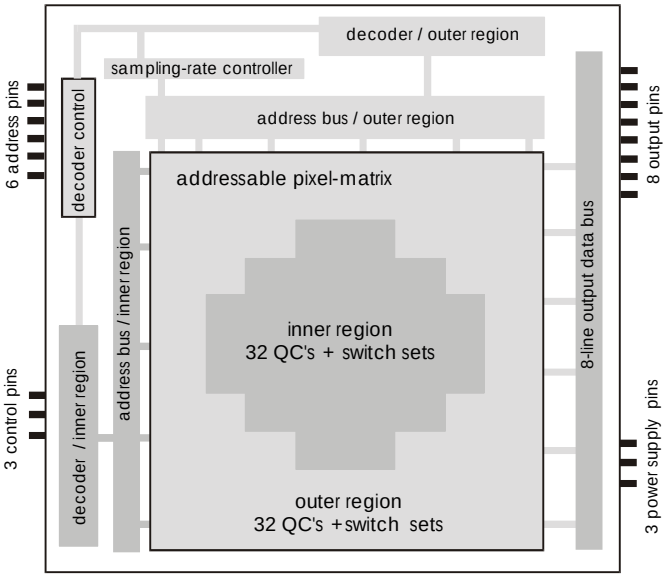

Fig. 3. Chip diagram with QC array, analog demux and sampling-rate controller.

The QC is 600μm x 600μm with a 14μm gap in between. The photon collection is read from both the shallow p^+/n-well and the 3μm deep n-well/p^--epilayer junctions, which form an almost overlapping depletion layer in order to improve the sensitivity to higher wavelengths in the visible spectrum.

The analog demultiplexer consists of a digital decoder and 256 on-pixel switch sets with compensating transmission gates. The decoder enables the pixels specified by the input address. Each switch set is either transmitting data to the output bus or otherwise discharging the accumulated pixel charge.

The sampling-rate controller is actually a two-state switch, which enables or blocks access to a number of amplifiers. When 8 outputs are enabled, the decoder requires only a 5-bit address and two QC's are addressed simultaneously.

V. Experimental Setup

We used a He-Ne laser, λ = 633 nm, passing by a pinhole to create a spherical wavefront, whose center is sampled by a ∅12mm entrance pupil. This portion of the wavefront is sampled by the Hartmann mask, which is placed 6 cm from the detector plane. At this distance the spot is radially symmetric and about 600 μm in diameter, with 90% of the intensity distribution confined within a 200μm radius. Since the wavelength is very small compared to the aperture, diffraction effects are negligible. The eight lines of the output bus are each connected to an operational amplifier in feedback mode, which performs a current-to-voltage conversion. The larger the gain, the larger the thermal noise contribution due to the feedback resistor.

VI. Discussion

The WFS performance is dependent on various parameters, including detector, data acquisition hardware, control, data-

handling and reconstruction algorithms. The data-acquisition hardware is described by the number of parallel acquisition channels, speed and analog-to-digital precision. The algorithms rely mainly on the raw data handling method, data fitting strategy, reconstruction method and its parameters. In this paper we focus on the detector performance.

The response of one fabricated QC, for a 600μm 5μW spot, can be seen in Fig. 4.

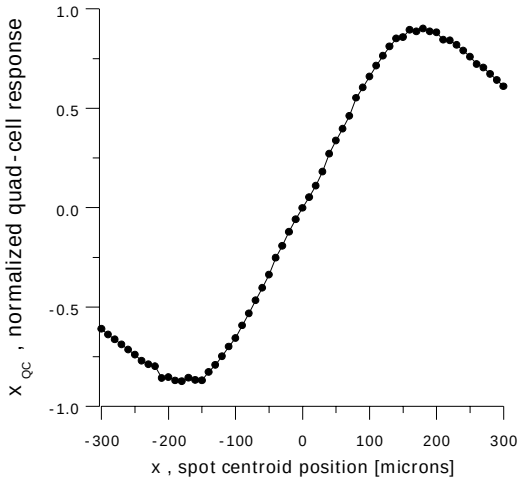

Fig. 4. Normalized response of the QC in the x-direction, for a 600μm 5μW radially symmetrical spot

It is a typical sigmoidal curve, described by (5), where the s_x parameter dictates the curve central slope and is dependent on the spot intensity profile.

$$x_{QC} = 1 - \frac{2}{\exp(x / s_x)} \tag{5}$$

The region that comprises 100 μm about the QC center features 99.6% linearity, which leads to 1.4 μm accuracy. As from (1) and (2), with f substituted by the distance D, between the Hartmann mask and the detector plane, an appropriate distance can be chosen so that the spot displacement lies within the QC linear region. Tilts generating displacements smaller than 1.4 μm will not be correctly detected. If the detector and mask are to be assembled as a single small unit, then distances higher than 10 cm are not suitable. A plot of local tilt versus the mask distance from the detector plane is displayed in fig.5.

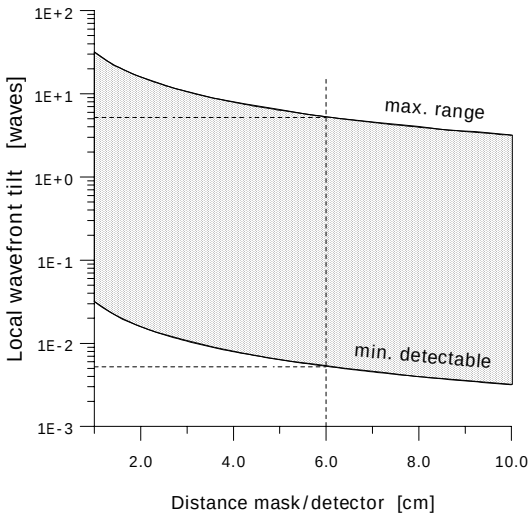

Fig. 5. The grayed region contains the allowed tilts for each distance between mask and detector. The upper curve limits the local tilt so that the spot centroid is kept within the linear region, whereas the lower curve determines the minimum accurately detectable tilt.

Noise can degrade readout signal. The main sources of noise are photoelectron noise, fixed-pattern noise (FPN), dark-current shot noise and circuit noise (including amplification) [9, 10]. Photoelectron noise is intrinsically related to the light intensity and the technology process characteristics, so there is not much we can do about it. Fixed-pattern noise arises from pixel doping level and transistor threshold voltage variations; as pixels are large, compensating transmission gates are used and no pixel buffers are present, this can be neglected. Dark-current is impossible to eliminate, but has its effects reduced by the use of a shallow p^+ layer.

Thus, the QC signal-to-noise ratio (SNR) depends basically on the intensity level and on noise introduced by the amplification stage. We found that the position SNR is 25dB for a 0.2μW spot, including amplification noise. This figure can be improved considerably if data is averaged. In absence of averaging, however, the minimum incident power to the wavefront sensor as a whole should not be less than about 100μW.

Each pixel has a junction capacitance and sheet resistance, which added to the switch set capacitance and wire capacitance and resistance determines its charge time. After switched on a completely discharged pixel takes 10μs to charge, which equals the switch-set settling time. The pixel access frequency is then 100KHz. When the sampling-rate controller is set to maximum speed (two QC's, 8 outputs, at a time), all WFS signals can be scanned with a frequency of 3.125KHz. This is more than what is usually required by most AO systems. The overall system frequency, however, will be reduced due to the data-acquisition and -processing and introduction of the adaptive corrector.

VII. Conclusions

We implemented a Hartmann wavefront sensor, with 8x8 position-sensitive detectors, in CMOS technology, which

makes integration of a variety of analog and digital electronic circuits on-chip feasible. So far an analog demultiplexer, switch sets and a sampling-rate controller have been added. An amplification stage and analog-to-digital conversion, among other functions, can be included further.

The detector features quad-cells with 99.6% linearity (position accuracy 1.4μm) and allows spot intensities as low as 0.2μW, as long as data is averaged. It was designed to accommodate scanning frequencies up to 3.125KHz. If operated along with optimized computer algorithms, the overall operational frequency will be suitable for real-time applications.

ACKNOWLEDGEMENTS

This project was supported by TU-Delft until December 2000, and since then it has been supported by the Dutch Technical Foundation STW (Project DOE 5375).

REFERENCES

[1] E. Fossum, "CMOS Image Sensors: Electronic Camera-On-A-Chip", *IEEE Trans. Electr. Devices*, vol. 44, no.10, pp.1689-1698, October 1997.

[2] R. Tyson, "Principles of Adaptive Optics", 2nd edition, Boston Academic Press, 1997.

[3] G. Vdovin and P. M. Sarro, "Flexible Mirror Micromachined in Silicon", *Applied Optics*, vol.*34*, pp.2968-2972, 1995.

[4] G. Vdovin et al., "Technology and Applications of Micromachined Silicon Adaptive Mirrors", *Optical Engineering*, vol.36, no.5, pp.1382-1390, 1997.

[5] J. M. Gaery, "Introduction to Wavefront Sensors", *SPIE\ Press*, 1995.

[6] D. Malacara, "Optical Shop Testing", 2nd edition, *John Wiley& Sons Inc.*, 1991.

[7] D. W. de Lima Monteiro et al., "Various layouts of analog CMOS optical position-sensitive detectors," *Proc. SPIE*, vol. 3794, pp.134-142, 1999.

[8] D. W. de Lima Monteiro et al., "Integration of a Hartmann-Shack wavefront sensor", *Proc. of Adaptive Optics Workshop for Industry and Medicine*, Durham – UK, pp.215-220, 1999.

[9] B. Saleh and M. Teich, "Fundamentals of Photonics", *John Wiley & Sons Inc.* , 1991.

[10]. S. K. Mendis et al, "CMOS Active Pixel Image Sensors for Highly Integrated Imaging Systems", *IEEE J. Solid-State Circuits*, vol.32, no.2, pp.187-197 February 1997.